CHEMICAL ENGINEERING TRANSACTIONS
VOL. 106, 2023
A publication of AIDIC
The Italian Association of Chemical Engineering
Online at www.cetjournal.it
Guest Editors: Jeng Shiun Lim, Nor Alafiza Yunus, Peck Loo Kiew, Hon Huin Chin

ISBN 979-12-81206-05-2; **ISSN** 2283-9216
DOI: 10.3303/CET23106014

Preparation, Characterization, and Carbon Dioxide Sorption Behaviour of Meranti Sawdust Porous Activated Carbon Using Taguchi L_9 Orthogonal Array

Nor Adilla Rashidi[a,*], Puteri Balqis Ahmad Hazmin[b], Leonardo Sambang[b]

[a]Chemical Engineering Department, Higher Institution Centre of Excellence - Centre for Biofuel and Biochemical Research, Institute of Self-Sustainable Building, Universiti Teknologi PETRONAS, 32610, Seri Iskandar, Perak, Malaysia
[b]Chemical Engineering Department, Universiti Teknologi PETRONAS, 32610, Seri Iskandar, Perak, Malaysia
adilla.rashidi@utp.edu.my

Emission of greenhouse gases is currently recognized as one of the most significant problems confronting societies all over the world. Human activities, such as the consumption of fossil fuels for the generation of heat and electricity, as well as other industrial operations and transportation, are the primary sources of greenhouse gas emissions. The implementation of adsorption technology for the capture of carbon are widely used to lower the greenhouse gas emissions mainly carbon dioxide (CO_2). However, there are still insufficient research has been done on the performance of Meranti sawdust as a low-cost carbon for CO_2 capture, particularly by using a greener activation agent. A mechanochemical activation method using potassium carbonate (K_2CO_3) is highlighted in this study, where the approach is simpler and more environmentally friendly. By using the Taguchi L_9 orthogonal array, several variables (i.e., temperature, impregnation ratio, duration, N_2 flow rate) have been investigated to determine the optimal operating conditions to obtain high yield activated carbon. From the findings, it is shown that the optimal conditions for the activated carbon production is at 700 °C, impregnation ratio of 3:1, carbonization time of 60 min, and N_2 flow of 900 mL/min, with corresponding activated carbon yield is approximately 41 % and CO_2 adsorption capacity of 2.8 mmol/g. The carbon materials are to be evaluated in terms of elemental composition, surface functionalities and morphologies, as well as textural characteristics. Overall, wood waste conversion to activated carbon aligns with SDG 9, SDG 12, as well as SDG 13.

1. Introduction

The global emissions of greenhouse gases particularly carbon dioxide (CO_2) from industrial and transportation sectors have become a serious issue presently due to the contribution towards the global warming issues. In 2020, it is reported that the average CO_2 concentration in the atmosphere is 412.5 ppm, which is 50 % higher than pre-industrialization times (Bhatt et al., 2023). The atmospheric CO_2 concentration is expected to double by 2050 (Bai et al., 2023). Hence, researchers worldwide have aggressively started to find the solutions to minimize the catastrophic impacts related to climate change. In context of CO_2 capture, it was reported that solid adsorption is a viable alternative to the existing chemical absorption technology, attributed to its process simplicity and low cost incurred (Zainol et al., 2021).The activated carbon is reported to be the most appropriate for CO_2 capture/separation since they are inexpensive, insensitive to moisture, high surface area, as well as high thermal stability (Singh and Kumar, 2016). Thus, research related to utilization of activated carbon for sustainable purposes is highly recommended. Hence, in this study, Meranti sawdust has been selected as starting material (precursors) for the activated carbon production since the material is one of the common forestry residues. In terms of physicochemical properties, the Meranti sawdust that is prone to biodegradation, has a hard structure and rich in carbon contents are promising characteristics for the activated carbon materials (Ahmad et al., 2020).

In terms of activated carbon production, chemical activation specifically using potassium hydroxide (KOH) has attracted many researchers due to moderate activation temperature, higher yield, as well as development of microporous structures with high specific surface area up to 3,000 m^2/g (Chen et al., 2020). Nevertheless, it is

Paper Received: 27 May 2023; Revised: 1 September 2023; Accepted: 12 September 2023
Please cite this article as: Rashidi N.A., Hazmin P.B.A., Sambang L., 2023, Preparation, Characterization, and Carbon Dioxide Sorption Behaviour of Meranti Sawdust Porous Activated Carbon Using Taguchi L9 Orthogonal Array, Chemical Engineering Transactions, 106, 79-84 DOI:10.3303/CET23106014

worth noting that KOH is not technically feasible due to its high corrosivity and possible equipment degradation, as well as high boiling temperature (1,327 °C) that results in chemical leftover upon the carbonization/activation process, in which will result in a significant danger to the environment (Singh et al., 2023). Therefore, current research has shifted to the use of greener chemicals, particularly potassium-based salts (other than KOH), has gained a significant attention. In this context, potassium carbonate (K_2CO_3) is being proposed as the alternative since it is a milder compound with less toxicity and corrosivity (Singh et al., 2023). It is important to note that the chemical reactions between K_2CO_3 and carbon precursors depends on several experimental conditions. In this research study, the Meranti sawdust-based activated carbon via K_2CO_3 activation is to be optimized in terms of carbonization temperature and duration, impregnation ratio, and inert flow rate. The Taguchi orthogonal array is adopted as the Design of Experiment, since it is capable to study multiple characteristics aspects and at the same time, to determine the most significant parameters of the process. Unlike the Response Surface Methodology, the Orthogonal array method allows an easier analysis with minimum number of experimental runs while the results are valid over the entire region spanned by the control factors (variables) and respective settings (Doraiselvan et al., 2015). Upon optimization, efficacy of the Meranti activated carbon in CO_2 adsorption at low and high temperature will be analysed. To date, there is scant literatures on the utilization of Meranti sawdust in gas phase adsorption. Momina et al. (2018) indeed reported that most of the work focused on the sawdust utilization in dyes removal, thus, infers to the novelty of this work. Besides, Nowicki and Pietrzak (2010) agreed that the porous sorbent obtained from this precursor is often found for the removal of pollutants from the liquid phase, while not many have investigated their potential in gas phase application.

2. Methodology

2.1 Materials

In this study, Meranti sawdust was purchased from a local industrial wood supplier as the activated carbon precursor. Potassium carbonate (K_2CO_3) was used as an activating agent in the activation of Meranti sawdust while the washing process was carried out by using the EMSURE 2M Hydrochloric Acid (HCl) (37 % purity). High purity nitrogen (N_2) and CO_2 gas were purchased from the Linde Malaysia Sdn. Bhd.

2.2 Synthesis of activated carbon

The Meranti sawdust was initially washed with distilled water to eliminate impurities that may affect the purity of the activated carbon, such as ash, dirt, and dust. Subsequently, the carbon feedstock was oven-dried at 105 °C overnight. The dried feedstock then was grinded and sieved to obtain the smaller particles, ranging from 100-500 um, before being kept in an airtight container. In terms of the activated carbon synthesis, one-step solid-solid mixing of powdered sawdust with K_2CO_3 at different ratio was carried out by using an automated ball milling machine. Upon completion, the mixture was placed in a ceramic crucible and placed in the horizontal tubular furnace. The activation process was carried out at temperatures of 700-900 °C for 1-2 h under N_2 flow rate of 300-900 mL/min. The detailed experimental design and analysis was done by using the Minitab® statistical software. Specifically, an L_9 orthogonal array was employed with a total of 9 experimental runs. Detailed synthesis of the Meranti Sawdust was summarized in Table 1. Upon completion of the activation process, the synthesized material was thoroughly washed with HCl and distilled water to remove the remaining chemicals, filtered, and oven-dried at 105 °C.

Table 1: Design of experiment with corresponding results

Run no.	Temp. (°C)	Impregnation ratio (wt./wt.)	Reaction time (min)	N_2 flowrate (mL/min)	Yield (%)	S/N ratio
1	700	1	60	300	31.8	30.05
2	700	2	120	600	36.2	31.17
3	700	3	240	900	29.4	29.37
4	800	1	120	900	34.6	30.78
5	800	2	240	300	24.4	27.75
6	800	3	60	600	36.8	31.32
7	900	1	240	600	17.8	25.01
8	900	2	60	900	37.0	31.36
9	900	3	120	300	31.6	29.99

2.3 Material characterizations

The functional groups present in the pristine sawdust and optimum activated carbon were evaluated by using a Frontier spectrometer at spectrum range of 4,000-400 cm^{-1}. Prior to analysis, these samples were mixed with potassium bromide followed by pressing into a pellet form. The surface morphology of these feedstock was evaluated by the ZEISS Microscopy coupled with Energy-Dispersive X-Ray Spectroscopy (EDX), while the surface and pore characteristics was determined via Micromeritics ASAP 2020. Prior to the measurement, the samples were degassed at 150 °C for 4 h to eliminate both moisture and contaminants residing in the pores. It has been reported that the EDX is a conventional method that allows the determination of elemental composition on the exterior of sample (Scimeca et al., 2018). To test the CO_2 adsorption performance at 25 °C and 100 °C, a static volumetric system (Particulate Matters HPVA-100) had been applied. The temperature was controlled via a Julabo recirculating water bath. Prior to measurement, the activated carbon was degassed under similar conditions, as previously mentioned. In a typical measurement, approximately 200 mg of these samples were weighed and inserted into the 2-cc sample holder, and then connected to instrument's analysis port via an OCR fitting. A sample gasket of 20-micron size was also placed on top of the sample holder to prevent the samples entering the manifold system.

3. Result and Discussions

3.1 Optimization of activated carbon production

The optimization of the activated carbon production with respect to carbon yield is evaluated in terms of Signal to Noise (S/N) ratio of 'the-larger-the-better' (Eq(1)), as this criterion refers to maximization of desired output. From Eq(1), *n* is the number of repeated runs for each experiment while *y* refers to the activated carbon yield (response). The experimental data is then transformed to S/N ratio, as summarized in Table 1. Based on the ranking of each factor as determined by the S/N ratio, it shows that the activation time is the most influential factor towards the activated carbon yield, followed by impregnation ratio, temperature, and lastly is the flow rate of inert N_2. Briefly, change in carbonization time along with temperature influences both dehydration and elimination reaction and cause pore wall destruction, subsequently, reduces the activated carbon yield. There is no substantial impact by the N_2 flowrate towards the activated carbon yield, as agreed by Bergna et al. (2020).

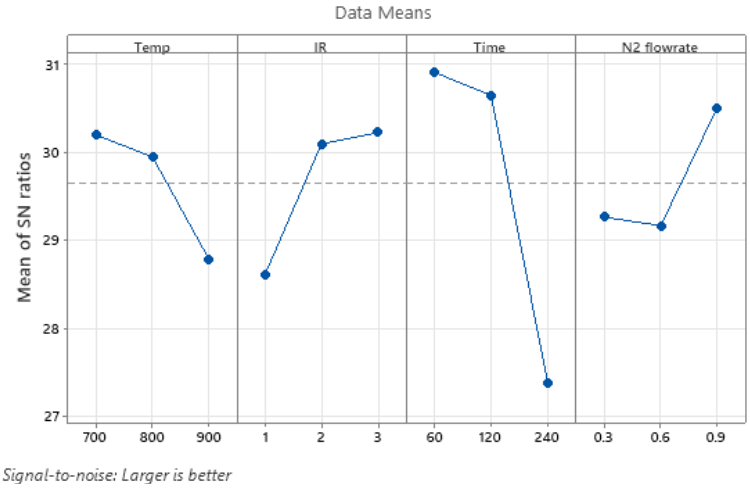

Figure 1: Main effects plot for S/N ratio.

From Figure 1, the optimum settings in producing high-yield activated carbon corresponds to the levels with the highest S/N ratio, based on the-larger-the-better algorithm. In other words, the optimum settings are observed at temperature of 700 °C (level 1), impregnation ratio of 3:1 (level 3), activation time of 60 min (level 1), and N_2 flowrate of 900 mL/min. By assuming that there is no interaction between the four control factors, the prediction of activated carbon yield at the optimum conditions can be calculated by using Eq(2).

$$\frac{S}{N}\ the-larger-the-better = -10log_{1o}\left(\frac{1}{n}\sum\frac{1}{Y^2}\right) \quad (1)$$

$$Optimum\ predicted = \bar{Y} + (\overline{A_1} - \bar{Y}) + (\overline{B_3} - \bar{Y}) + (\overline{C_1} - \bar{Y})(\overline{D_3} - \bar{Y}) \quad (2)$$

Referring to Eq(2), $\bar{Y}$ is the average activated carbon yield of all the experimental runs, $\overline{A_1}$ is the average activated carbon yield at optimum condition of activation temperature (Level 1), $\overline{B_3}$ is the average activated carbon yield at optimum condition of impregnation ratio (Level 3), $\overline{C_1}$ is the average activated carbon yield at optimum condition of activation time (Level 1) and $\overline{D_3}$ is the average activated carbon yield at optimum condition of N_2 flowrate during carbonization (Level 3). Upon substitution of the values at the respective conditions, the predicted yield is found to be 40.73 %. To validate this result, the activated carbon is then prepared at these optimum conditions, in which the average activated carbon yield is observed to be roughly 38 %. The deviation between predicted and experimental activated carbon that is below 10 % infers the significance of the Taguchi statistical model in this study (Levin et al., 2008).

3.2 Material characterization

Figure 2 displays the structural morphology of Meranti sawdust as well as the corresponding activated carbon at optimum settings. Referring to Figure 2, Meranti sawdust is a rough material with less fractures and voids, possibly due to aggregation of inorganic substances, which leads to a certain degree of pore blockage. On the other hand, the activated carbon structure is rather smooth with presence of pores and crevices, hence, verifies better porosity as compared to the starting material. According to Hamed et al. (2016), the formation of pores and cavities are the direct result of activating agent evaporating during the carbonization process. Specifically, K_2CO_3 activation in an inert atmosphere led to reduction in form of K, K_2O, CO_2, CO; at which the released K penetrates the structure of carbon matrix and subsequently widen the existing porosity while creating the new pores. Evaporation of K_2CO_3 results in cavities' production which are feasible to provide access to the adsorbate molecules to the interior structure of activated carbon (Heidarinejad et al., 2020). Presence of porosity upon the K_2CO_3 activation is further verified by the surface area and porosity analysis, as shown in Table 2. It is notably shown that the BET surface area and pore volume increase from 2.27 to 712.11 m^2/g, and 0.003 to 0.373 cm^3/g, respectively. From the findings, the microporous structure is dominant with fraction of almost 90 %, which is promising for the CO_2 adsorption. Rehman and Park (2019) reported that the presence of smaller micropores is favourable since they have been considered as preferential adsorption sites for CO2 molecules at 1 bar, and it will be filled to a high degree due to enhanced adsorption potential.

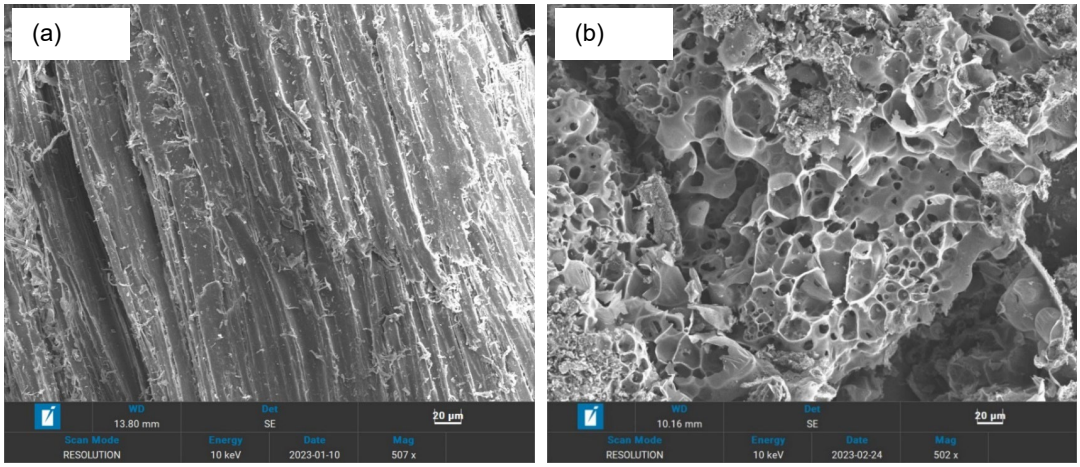

Figure 2: SEM images of (a) pristine Meranti sawdust and (b) optimum activated carbon.

The elemental composition of these materials has been evaluated as well, as summarized in Table 2. Upon activation, carbon content significantly increases while oxygen content reduces, as further supported by both elemental composition and FTIR analysis (Table 2). Specifically, for the raw sawdust, there are absence in O-functional groups upon K_2CO_3 activation process, hence, verifies the reduction in the oxygen content from 33.07 to 11.55 %. It has been reported that the absence of C=O groups is due to the bond cleavage caused by the activating agent, or heat treatment process in the activated carbon production (Yagmur et al., 2020). Likewise, disappearance of C-H bond upon the chemical activation is due to the breakage of weak bonds within the structure, which contributes to the reduction in hydrogen content. Overall, the liberation of volatile matters will increase the carbon content. Lastly, presence of potassium content in activated carbon may be caused by the leftover activating agent in the sample.

Table 2: Properties of pristine Meranti wood sawdust and activated carbon at optimum conditions.

Properties	Meranti Sawdust	Optimum activated carbon
Elemental composition (wt.%)		
Carbon	66.78	87.79
Oxygen	33.07	11.55
Calcium	0.14	0.07
Potassium	-	0.60
Surface area and pore characteristics		
BET surface area (m^2/g)	2.277	712.114
Micropore surface area (m^2/g)	-	642.40
Total pore volume (cm^3/g)	0.003	0.373
Average pore diameter	5.224	2.096
Functional groups		
O-H stretching	/	/
C-O stretching	/	/
C=O stretching	/	-
C=C stretching	/	-
C-H bending	/	-

3.3 CO_2 adsorption-desorption behavior

The CO_2 adsorption-desorption behaviour at 25 °C and 100 °C has been illustrated in Figure 3. Based on the findings, the reduction in CO_2 adsorption capacity at 100 °C compared to at ambient temperature signifies the CO_2 physisorption and exothermic behaviour. Such findings are consistent with literatures in which as the temperature increases, CO_2 molecules gain much higher kinetic energy that causes them to move faster and insufficient time to contact with the activated carbon's surface, hence, causes lesser adsorption capacity (Akpasi and Isa, 2022). Ba et al. (2023) agreed that the physisorbent materials are promising substitute to the conventional energy intensive process (chemisorbent material) due to lower energy consumption as well as milder operating condition. The physisorption nature could be supported by the overlapping between the adsorption and desorption curve. Moreover, increment in the CO_2 adsorption capacity is found to be parallel to the change in operating pressure.

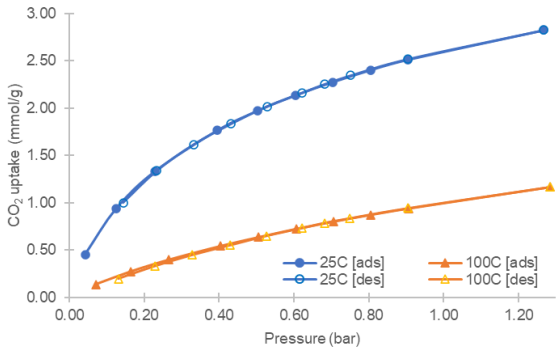

Figure 3: CO_2 adsorption-desorption on optimum activated carbon.

4. Conclusions

In conclusion, L_9 Taguchi Orthogonal Array design model in this study is reliable for the optimization of activated carbon production to produce maximum yield. The most influential factors towards the activated carbon yield are carbonization time, given the corresponding S/N ratio is the greatest when compared to the other variables. Specifically, the maximum activated carbon yield around 38 % is obtained at the following operational conditions: activation time of 60 min, impregnation ratio of 3:1, temperature of 700 °C, and N_2 flowrate of 0.9 L/min. The characterization of the optimum activated carbon indicates the presence of microporosity with BET surface area of 712 m^2/g, along with the increasing carbon contents upon the K_2CO_3 activation. The reduction in oxygen and hydrogen content upon the activation is supported by disappearance of several functional groups as well. In context of application, CO_2 adsorption capacity of around 2.8 mmol/g at room temperature that is higher than the reference commercial activated carbon indicates the feasibility of such carbonaceous material. The decline

in CO_2 uptake with respect to adsorption temperature signifies the exothermic and physisorption behaviour. Moving forward, it is recommended to carry out a life cycle as well as economic analysis of the proposed mechanochemical activation in this study, and to compare with the common impregnation technique used in chemical activation.

Acknowledgments

The research study is financially supported by Murata (Project no: RG2022-0755). In addition, we would like to acknowledge the Ministry of Higher Education Malaysia for providing the support and awarding the Higher Institution of Centre of Excellence (HICoE) status to the Centre of Biofuel and Biochemical, Universiti Teknologi PETRONAS.

References

Ahmad M.A., Yusop M.F.M., Tan S.H., 2020, Activated carbon from meranti wood sawdust waste prepared by microwave heating for dye removal, Advances in Waste Processing Technology, Chapter In: A. Yaser (ed.), Advances in Waste Processing Technology, Springer, Singapore, 61-87.

Akpasi S.O., Isa Y.M., 2022, Effect of operating variables on CO2 adsorption capacity of activated carbon, kaolinite, and activated carbon–Kaolinite composite adsorbent, Water-Energy Nexus, 5, 21-28.

Ba Y-Q, Wang Y-S, Li T-Y, Zheng Z., Hao G-P, Lu A-H, 2023, Fine tuning CO2 adsorption and diffusion behaviors in ultra-microporous carbons for favorable CO2 capture at moderate temperature, Sustainable Chemistry for Climate Action, 2, 100015.

Bai Y., Yang W., Zhu H., Jin J., Tian M., Hu Z., Shen L., 2023, Positive response of nitrite-dependent anaerobic methane oxidation to both gradual and abrupt increases of atmospheric CO2 concentration in paddy soils, Agriculture, Ecosystems & Environment, 343, 108291.

Bergna D., Hu T., Prokkola H., Romar H., Lassi U., 2020, Effect of some process parameters on the main properties of activated carbon produced from peat in a lab-scale process, Waste and Biomass Valorization 11, 2837-2848.

Bhatt H., Davawala M., Joshi T., Shah M., Unnarkat A., 2023, Forecasting and mitigation of global environmental carbon dioxide emission using machine learning techniques, Cleaner Chemical Engineering, 5, 100095.

Chen W., Gong M., Li K., Xia M., Chen Z., Xiao H., Fang Y., Chen Y., Yang H., Chen H., 2020, Insight into KOH activation mechanism during biomass pyrolysis: Chemical reactions between O-containing groups and KOH, Applied Energy, 278, 115730.

Doraiselvan K., Yusup S., Wai C.K., Muda N.S., 2015, Optimization studies on catalytic pyrolysis of empty fruit bunch (EFB) using L9 Taguchi orthogonal array, Chemical Engineering Transactions, 45, 1639-1644.

Hamed M.M., Ali M., Holiel M., 2016, Preparation of activated carbon from doum stone and its application on adsorption of 60Co and 152+154Eu: Equilibrium, kinetic and thermodynamic studies, Journal of Environmental Radioactivity, 164, 113-124.

Heidarinejad Z., Dehghani M.H., Heidari M., Javedan G., Ali I., Sillanpää M., 2020, Methods for preparation and activation of activated carbon: a review, Environmental Chemistry Letters, 18, 393-415.

Levin L., Herrmann C., Papinutti V.L., 2008, Optimization of lignocellulolytic enzyme production by the white-rot fungus Trametes trogii in solid-state fermentation using response surface methodology, Biochemical Engineering Journal, 39(1), 207-214.

Momina, Shahadat M., Isamil S., 2018, Regeneration performance of clay-based adsorbents for the removal of industrial dyes: a review, RSC advances, 8, 24571-24587.

Nowicki P., Pietrzak, R., 2010, Carbonaceous adsorbents prepared by physical activation of pine sawdust and their application for removal of NO2 in dry and wet conditions, Bioresource Technology, 101(15), 5802-5807.

Rehman A., Park S.J., 2019, Tunable nitrogen-doped microporous carbons: Delineating the role of optimum pore size for enhanced CO2 adsorption, Chemical Engineering Journal, 362, 731-742.

Scimeca M., Bischetti S., Lamsira H.K., Bonfiglio R., Bonanno E., 2018, Energy Dispersive X-ray (EDX) microanalysis: A powerful tool in biomedical research and diagnosis, European Journal of Histochemistry, 62(1), 2841.

Singh G., Ruban A.M., Geng X., Vinu A., 2023, Recognizing the potential of K-salts, apart from KOH, for generating porous carbons using chemical activation, Chemical Engineering Journal, 451, 139045.

Singh V.K., Kumar E.A., 2016, Measurement and analysis of adsorption isotherms of CO2 on activated carbon, Applied Thermal Engineering, 97, 77-86.

Yagmur E., Gokce Y., Tekin S., Semerci N.I., Aktas Z., 2020, Characteristics and comparison of activated carbons prepared from oleaster (Elaeagnus angustifolia L.) fruit using KOH and ZnCl2, Fuel, 267, 117232.

Zainol M.M., Hoe T.T., Yussuf M.A.M., Amin N.A.S., 2021, Carbon cryogel preparation via urea-furfural gel synthesis as an adsorbent for CO2 capture application, Chemical Engineering Transactions, 89, 187-192.